J|A|C|S COMMUNICATIONS

Published on Web 01/15/2010

Anodic Formation of Thick Anatase TiO_2 Mesosponge Layers for High-Efficiency Photocatalysis

Kiyoung Lee,[†] Doohun Kim,[†] Poulomi Roy,[†] Indhumati Paramasivam,[†] Balaji Ishwarrao Birajdar,[‡] Erdmann Spiecker,[‡] and Patrik Schmuki*,[†]

Department of Materials Science, WW4-LKO, University of Erlangen-Nuremberg, Martensstrasse 7, D-91058 Erlangen, Germany, and Department of Materials Science, WW7, University of Erlangen-Nuremberg, Cauerstrasse 6, D-91058 Erlangen, Germany

Received November 27, 2009; E-mail: schmuki@ww.uni-erlangen.de

Ever since the first report by Fujishima and Honda in 1972,[1] the unique photocatalytic properties of TiO_2 have attracted high and still increasing interest not only in the research community but also in view of technological applications such as self-cleaning or pollutant-degrading coatings.[2] The key to the high photocatalytic efficiency of TiO_2 lies in the semiconductive nature of its anatase structure, with a band gap of 3.2 eV and band-edge positions suitable to allow the formation of highly oxidative species from aqueous environments:[3] with UV light, electron−hole pairs can be created that in combination with water form $OH^{\bullet}$ radicals and peroxides on the TiO_2 surface. These radicals in turn are able to decompose virtually all hydrocarbon species[4] and thus can be exploited to degrade organic materials,[5] adjust the surface wettability,[4,6] establish antifogging properties,[7] or induce payload release by chain scission of attached monolayers.[4,8]

In order to achieve high photocatalytic conversion rates, a high specific TiO_2 surface area is typically desired. This can be attained by using nanoparticles (NPs) in suspensions or, as required in many applications, by immobilizing NPs on a substrate material. To produce such photoanodes, TiO_2 NPs (such as commercially available Degussa P25, with a BET surface area, A_{BET}, of ~50 m^2/g) are doctor-bladed or spin-coated onto a conductive substrate surface and compacted by adequate sintering.[9]

More recently, as an alternative for producing high-surface-area structures, self-organized TiO_2 nanotubes (NTs)[10] have been explored for photocatalytic applications.[11] These oxide layers can be grown on Ti sheets by a suitable electrochemical anodic treatment in fluoride-containing electrolytes and were shown to have a very high photocatalytic efficiency.[11a] However, a drawback in many TiO_2 nanostructure synthesis approaches is that the as-formed TiO_2 is amorphous, so a high-temperature treatment is required in order to form the photocatalytically much more active anatase structure.

In very recent work, we reported on an entirely novel anodization approach that forms a thick, amorphous, self-organized mesoporous oxide on Ti.[12] It is based on anodizing Ti in a hot glycerol K_2HPO_4 electrolyte followed by chemical etching of the structure.

Here we show that under modified anodization conditions, a titania mesosponge (TMS) structure can be formed that (i) provides a higher specific surface area than TiO_2 NTs, (ii) directly consists of anatase TiO_2 and thus provides a high photocatalytic activity as-formed, (iii) upon additional heat treatment exhibits an even higher photocatalytic activity than comparable P25 layers or TiO_2 NT layers, and (iv) provides mechanical robustness and flexibility.

Figure 1a shows an SEM cross section of a typical TMS layer formed by voltage-step anodization of a Ti metal foil at 50 V for 48 h in a 10 wt % K_2HPO_4-containing glycerol electrolyte followed by a chemical etch in 30 wt % H_2O_2 [see the Supporting Information (SI)].

The resulting structure shows uniform nanoporous channel morphology (with a "fishbone" structure) with 5−20 nm open channels and a scaffold width of 10−20 nm. The anodic oxide layer can easily be grown to different thicknesses (up to >10 μm) according to the holding times (two examples are shown in the insets of Figure 1a). These layers after formation consist directly of anatase or anatase/rutile mixtures (as evident from the HRTEM, SAD, and XRD data shown in Figure 1). Although it is known that extended anodization of Ti at high voltages can directly result in crystalline layers,[13] these layers are usually compact and limited to maximum thicknesses of some 100 nm.

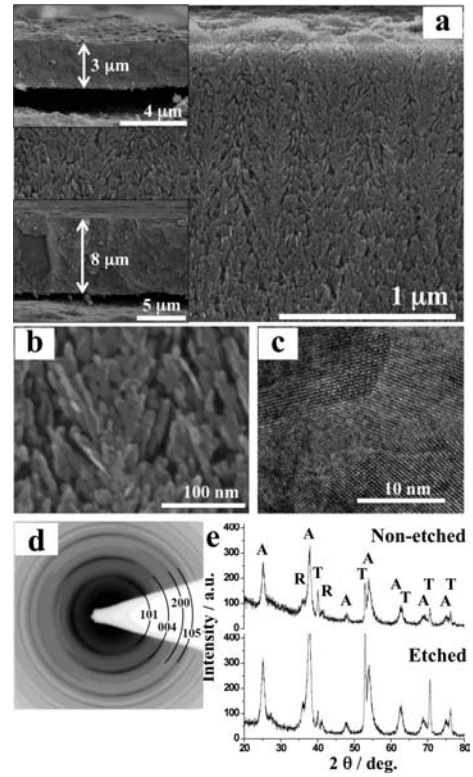

Figure 1. (a) SEM image of a TMS layer formed on Ti by anodization in 10 wt % K_2HPO_4 in glycerol at 180 ± 1 °C followed by etching in 30 wt % H_2O_2 for 7 h. A highly regular sponge morphology is apparent. The upper and lower insets show layers formed by anodization for 24 and 48 h, respectively. (b) Magnified SEM image of the layer morphology in (a). (c) HRTEM image and (d) SAD pattern of the layer in (a). (e) XRD patterns of samples before and after etching, respectively. The peaks are annotated as anatase (A), rutile (R), and Ti metal (T).

In the present case, for the as-formed TMS layers, XRD and HRTEM (shown in Figures S1 and S2 in the SI) reveal that the as-formed layer is porous and consists of anatase but still contains some amorphous material. When the layers are etched in 30 wt % H_2O_2, the chemical dissolution process preferentially removes amorphous paths present in the oxide layer (see the discussion of Figure S2 in the SI). Adjusting the etching time mainly affects the channel width (for different etching times from 0 to 7 h, the average channel width increased from 2−5 to 5−20 nm). Etching for times longer than 7 h led to partial disintegration of the sponge structure.

Figure 2 shows the kinetics for the photocatalytic decomposition of a model organic compound [Acid Orange 7 (AO7), a dye routinely used for determining the kinetics of photocatalytic decomposition reactions[14]] for differently prepared TMS layers.

[†] Department of Materials Science, WW4-LKO.
[‡] Department of Materials Science, WW7.

10.1021/ja910045x

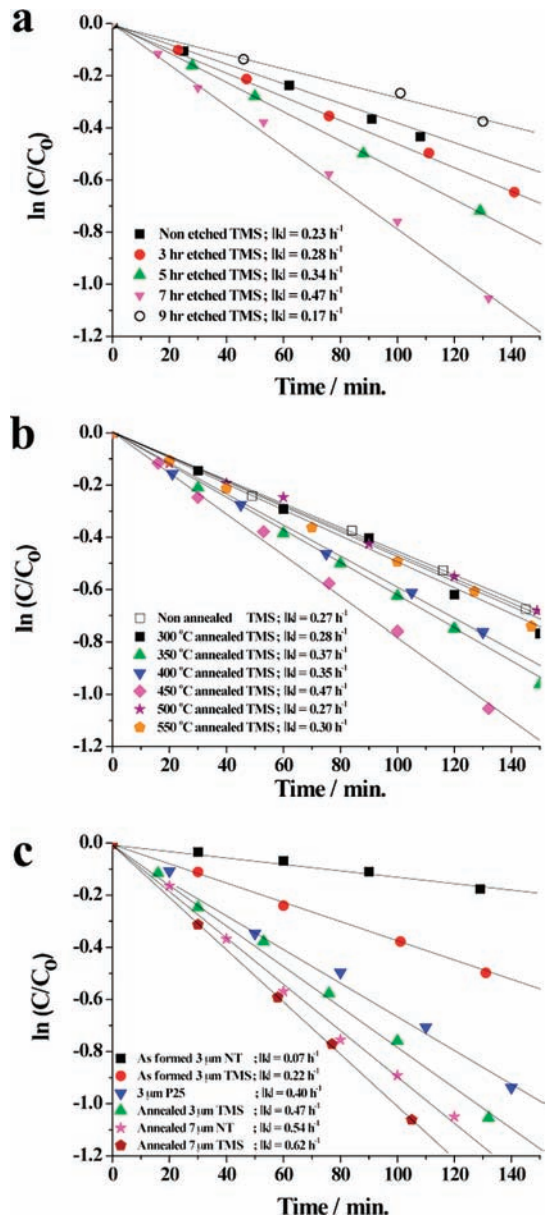

Figure 2. Comparison of photocatalytic decomposition rates of AO7 for TMS layers produced using (a) different etching durations in 30 wt % H_2O_2 (using a 3 μm TMS annealed at 450 °C for 3 h) and (b) different annealing temperatures of a 3 μm TMS etched in H_2O_2 for 7 h. (c) Comparison with other photocatalytic TiO_2 systems (3 μm thick P25, 7 μm long NTs). The TMS layers were annealed at 450 °C for 3 h and etched in H_2O_2 for 7 h. The straight lines are fits to a first-order rate law, and the corresponding rate constants are given in the figures.

Figure 2a clearly shows that the chemical etching process after layer formation is crucial for optimizing the photocatalytic activity, i.e., the sponge activity is increased with larger channel width, indicating a rate-controlling effect of reactant transport.[14] As mentioned above, the structure starts to degrade when etched for 9 h; therefore, a strong decrease in activity is observed.

From Figure 2b it is clear that although the as-formed structure already consists of a substantial amount of anatase, additional annealing under optimized conditions is beneficial to the photocatalytic activity of the mesospongeous material. According to XRD and TEM analyses, this can be ascribed to additional anatase formation and growth of anatase grains (see the SI). Annealing at temperatures higher than 450 °C is detrimental to the photocatalytic activity. At these temperatures, a significant amount of rutile formation takes place.

Figure 2c presents a comparison of TMS layers with other nanostructured photocatalytic electrode systems (TiO_2 NTs of comparable length and P25 layers of comparable thickness). It is evident that the high anatase content in the as-formed layer provides considerable photocatalytic activity even without any further annealing.

For the TMS layers, additional annealing clearly further improves the properties, and efficiencies even superior to those of P25 layers or annealed NT layers (converted under optimal conditions to anatase) can be obtained. This can be ascribed to two factors: First, a considerably higher specific surface area is provided by the TMS layers (A_{BET} = 78 m^2/g) than by NTs, where typically A_{BET} = 20−30 m^2/g is reported.[15] Second, in comparison with NP layers, the TMS layers provide direct interlinkage (the material is carved from a block by etching), while an optimized compacting of NPs often represents a considerable challenge and frequently results in nonideally interlinked NPs.

Under modified anodization conditions (potential sweeping to 50 V), samples can be grown to thicknesses of >50 μm (Figure S5). However, these as-formed layers are amorphous, have a different morphology, and even after annealing do not show a comparably high photocatalytic activity. Another very important advantage for practical applications is that the TMS layers provide very high mechanical adhesion to the substrate, are robust, and possess remarkable flexibility. For example, in a mechanical bending experiment, the TMS layer remained fully intact after bending to 170° (Figure S7); this contrasts with TiO_2 NT layers, which tend to flake off from the substrate during such a test).

Overall, it should be noted that many parameters of the anodization and etching process still need to be explored. However, it is already clear from the present first set of results that the mesospongeous TiO_2 material reported here shows a very high photocatalytic performance and is extremely promising for a full range of further applications where TiO_2 nanoscale substrates are used today.

Acknowledgment. The authors thank Helga Hildebrand and Dr. Himendra Jha for valuable technical help and acknowledge financial support from the DFG and the DFG Cluster of Excellence (EAM).

Supporting Information Available: HRTEM, crystallographic, photocatalytic, SEM, and optical images of the samples. This material is available free of charge via the Internet at http://pubs.acs.org.

References

(1) Fujishima, A.; Honda, K. *Nature* **1972**, *238*, 37.
(2) (a) Hoffmann, M. R.; Martin, S. T.; Choi, W.; Bahnemann, D. W. *Chem. Rev.* **1995**, *95*, 69. (b) Fujishima, A.; Zhang, X.; Tryk, D. A. *Surf. Sci. Rep.* **2008**, *63*, 515. (c) Linsebigler, A. M.; Lu, A.; Yates, J. T. *Chem. Rev.* **1995**, *95*, 735.
(3) Mills, A.; Davies, R. H.; Worsley, D. *Chem. Soc. Rev.* **1993**, *22*, 417.
(4) (a) Ohtsu, N.; Masahashi, N.; Mizukoshi, Y.; Wagatsuma, K. *Langmuir* **2009**, *25*, 11586. (b) Zubkov, T.; Stahl, D.; Thompson, T. L.; Panayotov, D.; Diwald, O.; Yates, J. T. *J. Phys. Chem. B* **2005**, *109*, 15454.
(5) (a) Turchi, C. S.; Ollis, D. F. *J. Catal.* **1990**, *122*, 178. (b) Zhang, F.; Zhao, J.; Shen, T.; Hidaka, H.; Pelizzetti, E.; Serpone, N. *Appl. Catal., B* **1998**, *15*, 147.
(6) Wang, R.; Sakai, N.; Fujishima, A.; Watanabe, T.; Hashimoto, K. *J. Phys. Chem. B* **1999**, *103*, 2188.
(7) Fujishima, A.; Rao, T. N.; Tryk, D. A. *J. Photochem. Photobiol., C* **2000**, *1*, 1.
(8) (a) Folkers, J. P.; Gorman, C. B.; Laibinis, P. E.; Buchholz, S.; Whitesides, G. M.; Nuzzo, R. G. *Langmuir* **1995**, *11*, 813. (b) Song, Y.-Y.; Schmidt-Stein, F.; Bauer, S.; Schmuki, P. *J. Am. Chem. Soc.* **2009**, *131*, 4230. (c) Shrestha, N. K.; Macak, J. M.; Schmidt-Stein, F.; Hahn, R.; Mierke, C. T.; Fabry, B.; Schmuki, P. *Angew. Chem., Int. Ed.* **2009**, *48*, 969.
(9) (a) Nakajima, A.; Hashimoto, K.; Watanabe, T.; Takai, K.; Yamauchi, G.; Fujishima, A. *Langmuir* **2000**, *16*, 7044. (b) Shrestha, N. K.; Macak, J. M.; Schmidt-Stein, F.; Hahn, R.; Mierke, C. T.; Fabry, B.; Schmuki, P. *Angew. Chem., Int. Ed.* **2009**, *48*, 969.
(10) (a) Ghicov, A.; Schmuki, P. *Chem. Commun.* **2009**, 2791. (b) Macak, J. M.; Tsuchiya, H.; Ghicov, A.; Yasuda, K.; Hahn, R.; Bauer, S.; Schmuki, P. *Curr. Opin. Solid State Mater. Sci.* **2007**, *11*, 3.
(11) (a) Macak, J. M.; Zlamal, M.; Krysa, J.; Schmuki, P. *Small* **2007**, *3*, 300. (b) Zlamal, M.; Macak, J. M.; Schmuki, P.; Krysa, J. *Electrochem. Commun.* **2007**, *9*, 2822. (c) Paramasivam, I.; Macak, J. M.; Schmuki, P. *Electrochem. Commun.* **2008**, *10*, 71.
(12) Kim, D.; Lee, K.; Roy, P.; Birajdar, B. I.; Spiecker, E.; Schmuki, P. *Angew. Chem., Int. Ed.* **2009**, *48*, 9326.
(13) Ohtsuka, T.; Guo, J.; Sato, N. *J. Electrochem. Soc.* **1986**, *133*, 2473.
(14) Kiriakidou, F.; Kondarides, D. I.; Verikios, X. E. *Catal. Today* **1999**, *54*, 119.
(15) (a) Jennings, J. R.; Ghicov, A.; Peter, L. M.; Schmuki, P.; Walker, A. B. *J. Am. Chem. Soc.* **2008**, *130*, 13364. (b) Roy, P.; Kim, D.; Lee, K.; Spiecker, E.; Schmuki, P. *Nanoscale* **2010**, *2*, 45.

JA910045X